Journal of Quantitative Spectroscopy & Radiative Transfer 310 (2023) 108745

Contents lists available at ScienceDirect

Journal of Quantitative Spectroscopy and Radiative Transfer

journal homepage: www.elsevier.com/locate/jqsrt

Line lists for TiO minor isotopologues for the $A^3\Phi$-$X^3\Delta$ electronic transition

P. Bernath [a,b,*], D. Cameron [b]

[a] Department of Chemistry, Old Dominion University, Norfolk, VA, United States
[b] Department of Physics, Old Dominion University, Norfolk, VA, United States

ARTICLE INFO

Keywords:
Molecular data – opacity – astronomical databases
Exoplanets-atmospheres
Stars-brown dwarfs
TiO isotopic species
Molecular constants
Molecular line lists

ABSTRACT

The TiO $A^3\Phi$-$X^3\Delta$ electronic transition (γ system) is a significant opacity source in M dwarf stars as well as in the atmospheres of hot Jupiter exoplanets. The minor isotopologues, ^{46}TiO, ^{47}TiO, ^{49}TiO and ^{50}TiO, specifically the 0–0 and 0–1 bands, have been analyzed, producing spectroscopic constants for the $A^3\Phi$ ($v = 0$) state and line lists with line positions based on experiment. In total 8248 lines in the $A^3\Phi$-$X^3\Delta$ transition were fitted, with wavenumbers ranging from 12,827 cm^{-1} to 14,172 cm^{-1} (780–706 nm) with J values from 1 to 70. The TiO emission spectrum used for the analysis was recorded at the McMath-Pierce Solar Telescope, operated by the National Solar Observatory at Kitt Peak, Arizona.

1. Introduction

TiO is among the most prominent diatomic molecules from an astronomical perspective, given the early discovery of its spectral lines by Fowler in 1907 [1] and its strong presence in the visible and near infrared spectra of M dwarf stars [2]. The significance of TiO has increased with the exploration of exoplanets, where TiO has been shown to cause formation of stratospheres in hot Jupiters [3,4]. Recent analysis of observations of oxygen-rich asymptotic giant branch (AGB) stars have revealed a significant presence of TiO as a possible precursor to dust [5]. Astronomical observations of TiO need to be supported by comprehensive line lists, which should be based on laboratory spectroscopy. The ExoMol TiO line list by McKemmish et al. [6] is currently the most comprehensive and reliable, with 30 million ^{48}Ti^{16}O transitions as well as predictions for the four minor isotopologues, derived for titanium's four minor isotopes: ^{46}Ti, ^{47}Ti, ^{49}Ti and ^{50}Ti with natural abundances on Earth of 8%, 7%, 5% and 5%, respectively. The ExoMol line list is calculated from potential energy curves using the DUO program [7]. The potential energy curves were adjusted using experimental data and calculated line positions were replaced by calculated values from experimentally derived term values, if available.

A thorough summary of TiO laboratory spectroscopy for the ^{48}Ti^{16}O molecule was made by McKemmish et al. [8]. Since then, our group has continued to improve TiO laboratory spectroscopy; those efforts include analysis of singlet transitions [9], the $C^3\Delta$ -$X^3\Delta$ transition [10], absorption cross sections in the visible and near IR [11], the $E^3\Pi$ -$X^3\Delta$ transition [12] and the $B^3\Pi$ -$X^3\Delta$ transition [13].

The isotopes of Ti have different nucleosynthetic origins: oxygen and silicon burning in massive stars yields ^{46}Ti and ^{47}Ti, $^{48-50}$Ti are formed mainly in supernova explosions [14]. Determining the relative abundances of isotopes and understanding the processes that form the various isotopes can potentially lead to determining the formation and evolution of astronomical objects [15]. The relative abundances of Ti isotopes of two M dwarf stars were measured by Pavlenko et al. [16] using the ExoMol line list. They found that $^{46-48}$Ti abundances were reduced by a few % and $^{49-50}$Ti abundances were increased by a few% relative to solar abundances. Current large telescopes with high resolution spectrographs such as the VLT/RISTRETTO and those coming such as the ELT/ANDES can determine the relative TiO abundances of young gas giant exoplanets [15]. We present here the results of rotational analysis of the minor TiO isotopologues, through laboratory spectroscopy, providing improvement to existing experimental line lists.

2. Method and results

The rotational analysis of the minor isotopologues of the TiO molecule $A^3\Phi$-$X^3\Delta$ transition was carried out with the PGOPHER program [17], using as an overlay the same TiO experimental cross sections, recorded at McMath-Pierce Solar Telescope at Kitt Peak, AZ in 1985, that were used by Bernath and Cameron [12] and Cameron and Bernath [13]. The source for the emission spectrum is a carbon tube furnace operated at about 2300 K; the conversion of the spectrum to calibrated

* Corresponding author at: Department of Chemistry, Old Dominion University, Norfolk, VA, United States.
E-mail address: pbernath@odu.edu (P. Bernath).

https://doi.org/10.1016/j.jqsrt.2023.108745
Received 16 February 2023; Received in revised form 13 June 2023; Accepted 1 August 2023
Available online 2 August 2023

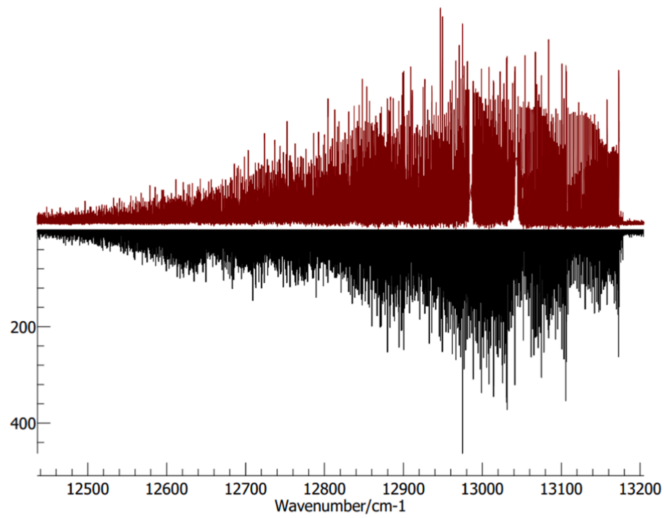

Fig. 1. TiO spectrum, a portion of the $A^3\Phi$-$X^3\Delta$ transition 0–1 band, in red pointing upwards, simulation pointing downwards.

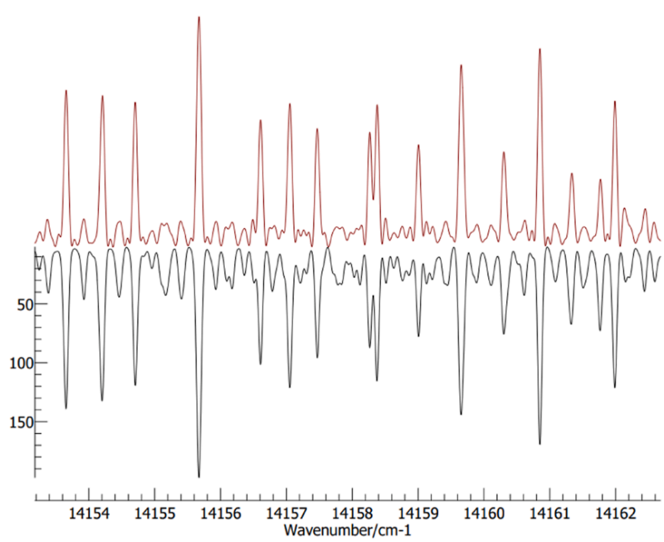

Fig. 2. TiO spectrum, an expanded portion of the $A^3\Phi$-$X^3\Delta$ transition, 0–0 band, highlighting the accuracy of the simulation, pointing downwards.

cross sections is detailed by Bernath [11]. Wavenumber calibration accuracy for the cross sections is ±0.002 cm^{-1} and the spectral resolution is about 0.05 cm^{-1}. In addition, low J-line positions for the 0–0 band of all four minor isotopologues from Barnes et al. [18] were manually added to the PGOPHER fit.

The states in the $A^3\Phi$-$X^3\Delta$ transition obey Hund's case (a) coupling; each vibrational band has 3 subbands due to the three spin components, and each subband has P, Q and R branches, with no Λ-doubling. Fig. 1 shows an overview of the 0–1 band; the cross sections are in red, pointing up, and the simulation is pointing down. Fig. 2 shows an expanded portion of the 0–0 band, allowing a better view of the faithfulness of the simulation. In general, the stronger lines are generated by the main ^{48}Ti^{16}O isotopologue, and the weaker lines are from the minor isotopologues, as demonstrated in Fig. 3, where the main isotopologue simulation is pointing downwards in black, and the minor isotopologues are color coded as described in the figure caption. Note the line strengths in Fig. 1 through 4 were set manually in PGOPHER to match the line strengths of the cross sections, not calculated. The most prominent feature in Fig. 3, at 14,155.7 cm^{-1}, is expanded in Fig. 4 to get a better sense of the distribution of the lines of the different isotopologues. The

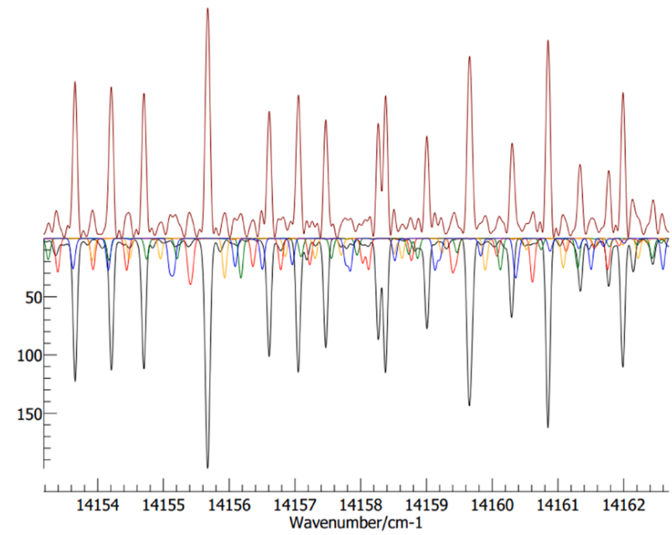

Fig. 3. The same portion of the $A^3\Phi$-$X^3\Delta$ transition, 0–0 band, depicted in Fig. 2, with color coding added to show the isotopologues that comprise the features. Blue is ^{46}Ti^{16}O, red is ^{47}Ti^{16}O, black is ^{48}Ti^{16}O, orange is ^{49}Ti^{16}O and green is ^{50}Ti^{16}O.

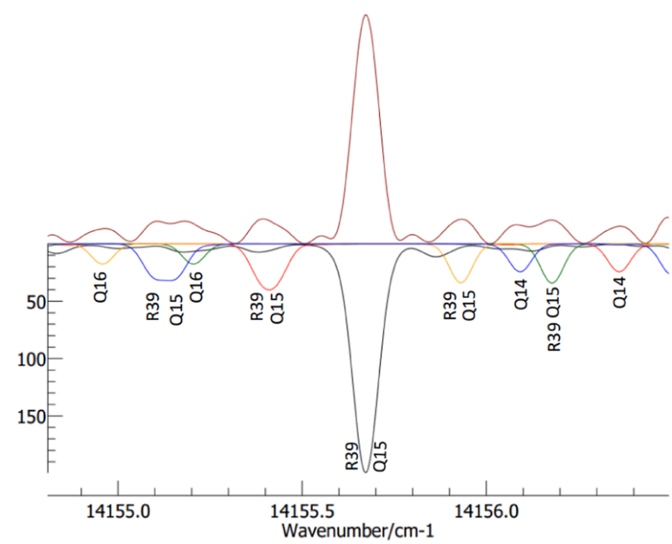

Fig. 4. Expanded view of the prominent feature in Fig. 3 at 14,155.7 cm^{-1}. Lines composing the features are labelled. Color coding as in Fig. 3.

same color scheme introduced in Fig. 3 is continued in Fig. 4. It can be seen the feature at 14,155.7 stands out because it is a merger of two lines of the major ^{48}Ti^{16}O isotopologue, specifically an R(39) line and a Q(15) line. It can be seen that the same two lines are merged into a single feature for all five isotopologues, which appear in order by mass starting with the ^{46}Ti^{16}O isotopologue on the left progressing through the ^{50}Ti^{16}O isotopologue on the right. In the rotational analysis, 8233 lines from the 0–0 and 0–1 bands were fit across the four minor isotopologues with an average observed minus calculated error of 0.013 cm^{-1}. These observed lines are provided in Supplementary Table 1.

To begin the analysis, initial spectroscopic constants for both the $A^3\Phi$ and $X^3\Delta$ states for the major ^{48}Ti^{16}O isotopologue were obtained from Ram et al. [19]. Ram et al. [19] provide equilibrium constants as a power series. These equilibrium constants were scaled for the different atomic masses of the four minor isotopologues using the following usual relationship from Bernath [20]:

Table 1
Equilibrium constants for the TiO minor isotopologues for $X^3\Delta$ and $A^3\Phi$ states in cm^{-1} derived from the Ram et al. [19] $^{48}Ti^{16}O$ constants, which are included for reference. The Ram et al. [19] format has been replicated: $P_v = \sum_{k=0}^{3} p_k \left(v + \frac{1}{2}\right)^k$. For $P_v = T_v, p_0 = T_e, p_1 = \omega_e, p_2 = -\omega_e x_e, p_3 = \omega_e y_e$; for $P_v = B_v, p_0 = B_e, p_1 = -\alpha_e, p_2 = \gamma_e$ etc.

P_v	p_0	p_1	p_2	p_3
$^{46}Ti^{16}O$ $X^3\Delta$ State				
T_v	0	1014.642232	−4.611283418	−3.843378E-03
B_v	0.541149919	−0.003073155	−9.4132E-06	0
D_v	6.15486E-07	3.50849E-09	3.30541E-11	0
H_v	7.10663E-14	0	0	0
A_v	50.650414	0.001944475	−8.852114E-04	0
A_{Dv}	−2.61946E-05	−1.1199E-06	0	0
λ_v	1.749911	−0.005449355	3.031574E-04	0
λ_{Dv}	6.79703E-07	0	0	0
$^{46}Ti^{16}O$ $A^3\Phi$ State				
T_v	14,163.554562	872.215449	−3.875084	−0.011903
B_v	5.128105E-01	−0.003218	−5.8797E-06	−3.5342E-07
D_v	7.082973E-07	1.119223E-09	1.7994E-10	0
H_v	1.180650E-13	0	0	0
A_v	58.010058	−1.064333E-01	0.001214	0
A_{Dv}	−4.246629E-05	2.640442E-07	0	0
λ_v	−5.163460E-01	3.068530E-03	−0.000249	0
λ_{Dv}	−4.534320E-06	1.965595E-07	0	0
$^{47}Ti^{16}O$ $X^3\Delta$ State				
T_v	0	1011.850914	−4.585946703	−0.003811745
B_v	0.538176569	−3.047862E-03	−9.31004E-06	0
D_v	6.08741E-07	3.46049E-09	3.25122E-11	0
H_v	6.99013E-14	0	0	0
A_v	50.650414	1.939125E-03	−8.803476E-04	0
A_{Dv}	−2.60506E-05	−1.11068E-06	0	0
λ_v	1.749911	−5.434364E-03	3.014917E-04	0
λ_{Dv}	6.75969E-07	0	0	0
$^{47}Ti^{16}O$ $A^3\Phi$ State				
T_v	14,163.554562	869.815953	−3.853792	−1.180466E-02
B_v	5.099929E-01	−3.191863E-03	−5.815239E-06	−3.485825E-07
D_v	7.005352E-07	1.103912E-09	1.769884E-10	0
H_v	1.161296E-13	0	0	0
A_v	58.010058	−1.061405E-01	1.207676E-03	0
A_{Dv}	−4.223296E-05	2.618710E-07	0	0
λ_v	−5.163460E-01	3.060088E-03	−2.480093E-04	0
λ_{Dv}	−4.509407E-06	1.949417E-07	0	0
Terms in parentheses for the source main $^{48}Ti^{16}O$ isotopologue equilibrium constants are 1 standard deviation.				
$^{48}Ti^{16}O$ $X^3\Delta$ State				
T_v	0	1009.176435(654)	−4.561736(301)	−3.7816(420)E-03
B_v	0.535335360(164)	−3.023758(366)E-03	−9.2120(912)E-06	0
D_v	6.023307(870)E-07	3.4150(632)E-09	3.20(180)E-11	0
H_v	6.88(161)E-14	0	0	0
A_v	50.650414(100)	1.934(166)E-03	−8.757(350)E-04	0
A_{Dv}	−2.59131(267)E-05	−1.1019(524)E-06	0	0
λ_v	1.749911(138)	−5.420(258)E-03	2.999(568)E-04	0
λ_{Dv}	6.724(158)E-07	0	0	0
$^{48}Ti^{16}O$ $A^3\Phi$ State				
T_v	14,163.554562(548)	867.516894(914)	−3.833447(453)	−1.17113(623)E-02
B_v	0.507300491(369)	−3.166620(701)E-03	−5.754(322)E-06	−3.440(406)E-07
D_v	6.931580E-07(107)	1.0894(805)E-09	1.742(265)E-10	0
H_v	1.143(168)E-13	0	0	0
A_v	58.0100584(943)	−0.1058600(935)	1.2013(169)E-03	0
A_{Dv}	−4.20100(328)E-05	2.598(324)E-07	0	0
λ_v	−0.516346(226)	3.052(234)E-03	−2.467(441)E-04	0
λ_{Dv}	−4.4856(813)E-06	1.934(546)E-07	0	0
$^{49}Ti^{16}O$ $X^3\Delta$ State				
T_v	0	1006.594674	−4.538425415	−3.752651E-03
B_v	0.532599783	−3.000610E-03	−9.118093E-06	0
D_v	5.96191E-07	3.37154E-09	3.15119E-11	0
H_v	6.77507E-14	0	0	0
A_v	50.650414	1.929052E-03	−8.712252E-04	0
A_{Dv}	−2.57807E-05	−1.09346E-06	0	0
λ_v	1.749911	−5.406134E-03	2.983675E-04	0
λ_{Dv}	6.68964E-07	0	0	0
$^{49}Ti^{16}O$ $A^3\Phi$ State				
T_v	14,163.554562	865.297539	−3.813858	−1.162165E-02
B_v	0.504708	−3.142379E-03	−5.695344E-06	−3.396222E-07
D_v	6.860920E-07	1.075536E-09	1.715431E-10	0
H_v	1.125567E-13	0	0	0
A_v	58.010058	−0.105589	1.195161E-03	0
A_{Dv}	−4.179533E-05	2.578112E-07	0	0
λ_v	−0.516346	3.044192E-03	−2.454394E-04	0
λ_{Dv}	−4.462678E-06	1.919195E-07	0	0
$^{50}Ti^{16}O$ $X^3\Delta$ State				
T_v	0	1004.11736	−4.516114009	−3.725012E-03
B_v	0.529981463	−2.978511E-03	−9.02866E-06	0
D_v	5.90343E-07	3.33026E-09	3.10495E-11	0
H_v	6.67564E-14	0	0	0
A_v	50.650414	1.924305E-03	−8.669421E-04	0
A_{Dv}	−2.56539E-05	−1.085411E-06	0	0
λ_v	1.749911	−5.392829E-03	2.969007E-04	0
λ_{Dv}	6.65675E-07	0	0	0
$^{50}Ti^{16}O$ $A^3\Phi$ State				
T_v	14,163.554562	863.167968	−3.795109	−1.153605E-02
B_v	0.502227	−3.119235E-03	−5.639484E-06	−3.354635E-07
D_v	6.793628E-07	1.062366E-09	1.690256E-10	0
H_v	1.109048E-13	0	0	0
A_v	58.010058	−0.105329	1.189286E-03	0
A_{Dv}	−4.158986E-05	2.559124E-07	0	0
λ_v	−5.163460E-01	3.036700E-03	−2.442327E-04	0
λ_{Dv}	−4.440739E-06	1.905060E-07	0	0

$$Y_{jk} \propto \mu^{-(j+2k)/2}, \tag{1}$$

in which Y_{jk} is a Dunham parameter and μ is the reduced mass.

Bernath [20] also details the relationship between Dunham parameters and conventional spectroscopic constants using customary energy level expressions to obtain the origin, B, D, and H constants. The A, A_D, λ and λ_D spin-orbit and spin-spin initial constants were obtained from similar Dunham-like expansion parameters provided by Ram et al. [19]. There is no isotopic dependence for A or λ, but A_D and λ_D were scaled with the same isotopic dependence as *B*. The derived equilibrium constants are shown in Table 1.

The equilibrium constants were used to generate initial values for the spectroscopic constants for $v = 0$ through $v = 4$ for both the $A^3\Phi$ and $X^3\Delta$ states (Supplementary Table 2). These initial constants were used to start the analysis of the isotopologue lines in the 0–0 and 0–1 bands. The ground state constants were held fixed to the calculated values in Table 2 and Supplementary Table 2, and the $v = 0$ $A^3\Phi$ constants were fitted. Updated $A^3\Phi$ spectroscopic constants for $v = 0$ derived from the PGOPHER rotational analysis are shown in Table 3. A line list was calculated for all the isotopologues for the 0–0, 0–1, 0–2, 0–3 The line list table is available with a separate table for each isotopologue, in total containing 183,212 lines.

The equilibrium vibrational and rotational constants (Table 1) were also input into LeRoy's Rydberg-Klein-Rees (RKR) program [21] to

Table 2
Table 2 is the calculated spectroscopic constants for $A^3\Phi$ $v = 0$. The complete set of calculated spectroscopic constants are provided in Supplementary Table 2.

	$^{46}Ti^{16}O$	$^{47}Ti^{16}O$	$^{48}Ti^{16}O$	$^{49}Ti^{16}O$	$^{50}Ti^{16}O$
T	14,092.5242	14,092.7191	14,092.9059	14,093.0861	14,093.2591
B	0.5111999	0.5083955	0.5057157	0.4999806	0.5006659
D	7.089019E-07	7.011314E-07	6.937463E-07	6.880913E-07	6.799362E-07
H	1.180650E-13	1.161296E-13	1.143000E-13	1.125567E-13	1.109048E-13
A	57.95715	57.95729	57.95743E	57.85436	57.95769
A_D	−4.233427E-05	−4.210203E-05	−4.188010E-05	−4.140861E-05	−4.146190E-05
λ	−0.5148741	−0.5148780E	−0.5148817	−0.5123320	−0.5148887
$λ_D$	−4.436041E-06	−4.411936E-06	−4.388900E-06	−4.174799E-06	−4.345486E-06

Table 3
Spectroscopic constants for the $v = 0$ $A^3\Phi$ state of the minor isotopologues of TiO in cm^{-1} obtained from rotational analysis. The major isotopologue $^{48}Ti^{16}O$ constants are from Ram et al. [19] and included for reference. Terms in parentheses are 1 standard deviation.

	$^{46}Ti^{16}O$	$^{47}Ti^{16}O$	$^{48}Ti^{16}O$	$^{49}Ti^{16}O$	$^{50}Ti^{16}O$
T	14,092.47573(73)	14,092.70196(74)	14,092.905684(193)	14,093.10467(74)	14,093.29833(76)
B	0.5112005(16)	0.5083876(16)	0.505716075(244)	0.5031484(16)	0.5006448(16)
D	7.1031(80)E-7	6.9804(80)E-7	6.937508(942)E-7	6.9349(80)E-7	6.6164(81)E-7
H	3.9(11)E-13	−1.5(11)E-13	8.25(102)E-14	9.9(11)E-13	−2.96(11)E-12
A	57.95700(18)	57.95680(16)	57.9573454(742)	57.95792(18)	57.96225(19)
A_D	−4.2117(79)E-5	−4.1542(79)E-5	−4.18140(290)E-5	−4.1320(80)E-5	−4.2521(81)E-5
λ	−0.51486(49)	−0.51359(49)	−0.515184(168)	−0.51472(49)	−0.51313(50)
$λ_D$	−5.32(23)E-6	−5.31(23)E-6	−4.2199(692)E-6	−5.67(23)E-6	−7.17(23)E-6

Table 4
Transition-dipole Moment Matrix Elements for TiO $A^3\Phi$-$X^3\Delta$ Transition.

Band	Transition-dipole Moment Matrix Element (debye)				
v′ – v″	$^{46}Ti^{16}O$	$^{47}Ti^{16}O$	$^{48}Ti^{16}O$	$^{49}Ti^{16}O$	$^{50}Ti^{16}O$
0–0	2.07264	2.07149	2.07091	2.07053	2.06635
0–1	1.02271	1.02440	1.02546	1.02628	1.03152
0–2	3.56732E-1	3.58126E-1	3.59009E-1	3.59710E-1	3.62588E-1
0–3	9.71877E-2	9.78218E-2	9.82541E-2	9.86166E-2	1.00568E-1
0–4	2.16345E-2	2.17894E-2	2.19642E-2	2.21422E-2	2.28013E-2

Table 5
Calculated TiO $X^3\Delta$ $v = 0$ state spectroscopic constants compared with Lincowski et al. [23] in cm^{-1}. Numbers in parentheses are 1 standard deviation.

	Calculated	Lincowski et al. [23]
$^{46}Ti^{16}O$		
B	0.5396110	0.539608942(21)
D	6.172487E-07	6.17727E-07(56)
A_D	−2.675451E-05	−2.73022E-05(47)
$λ_D$	6.797033E-07	6.288E-07(83)
$^{47}Ti^{16}O$		
B	0.5366503	0.536649311(22)
D	6.104796E-07	6.10686E-07(63)
A_D	−2.660597E-05	−2.68983E-05(57)
$λ_D$	6.759687E-07	7.23E-07(26)
$^{49}Ti^{16}O$		
B	0.5310972	0.531098327(19)
D	5.978842E-07	5.98301E-07(32)
A_D	−2.632742E-05	−2.61548E-05(47)
$λ_D$	6.689640E-07	6.32E-07(11)
$^{50}Ti^{16}O$		
B	0.5284900	0.528492094(24)
D	5.920160E-07	5.92513(60)E-07
A_D	−2.619665E-05	−2.58065(53)E-05
$λ_D$	6.656753E-07	6.104(97)E-07

generate potential energy curves for the A and X states of all isotopologues. The potential energy curves, along with the transition dipole moment for the $A^3\Phi$-$X^3\Delta$ transition, obtained from McKemmish et al. [6] Fig. 4 and Eq. (4), were then input into LeRoy's LEVEL program [22], which generated transition-dipole moment matrix elements, shown in Table 4.

Table 6
Comparison of equilibrium constants for the TiO $X^3\Delta$ state (cm^{-1}). The equivalent Dunham parameter symbol is shown in parentheses next to the equilibrium constant symbol in the first column.

	Breier et al. [24]	Witsch et al. [25]	Calculated (this work)
$^{46}Ti^{16}O$			
ω_e (Y_{10})	1014.641593	1014.639822	1014.642261
$\omega_e x_e$ ($-Y_{20}$)	4.610977103	4.610454558	4.611283418
B_e (Y_{01})	0.541314542	0.54131547	0.541149932
α_e ($-Y_{11}$)	0.003072747	0.003072671	0.003073155
γ_e (Y_{21})	−9.56609E-06	−9.47517E-06	−9.4132E-06
$^{47}Ti^{16}O$			
ω_e (Y_{10})	1011.850278	1011.848511	1011.850943
$\omega_e x_e$ ($-Y_{20}$)	4.585642071	4.585122397	4.585946703
B_e (Y_{01})	0.538340288	0.53834121	0.538176582
α_e ($-Y_{11}$)	3.04745722E-03	3.04738199E-03	3.04786210E-03
γ_e (Y_{21})	−9.46126E-06	−9.37133E-06	−9.31004E-06
$^{48}Ti^{16}O$			
ω_e (Y_{10})	1009.1758	1009.174038	1009.176464
$\omega_e x_e$ ($-Y_{20}$)	4.561432976	4.560916046	4.561736
B_e (Y_{01})	0.535498214	0.535499131	0.535335373
α_e ($-Y_{11}$)	3.02335632E-03	3.02328169E-03	3.02375800E-03
γ_e (Y_{21})	−9.36162E-06	−9.27264E-06	−9.2120E-06
$^{49}Ti^{16}O$			
ω_e (Y_{10})	1006.594041	1006.592284	1006.594703
$\omega_e x_e$ ($-Y_{20}$)	4.538123939	4.537609651	4.538425415
B_e (Y_{01})	0.532761805	0.532762717	0.532599796
α_e ($-Y_{11}$)	3.00021181E-03	3.00013775E-03	3.00061042E-03
γ_e (Y_{21})	−9.26619E-06	−9.17812E-06	−9.11809E-06
$^{50}Ti^{16}O$			
ω_e (Y_{10})	1004.116728	1004.114975	1004.117388
$\omega_e x_e$ ($-Y_{20}$)	4.515814015	4.515302255	4.516114009
B_e (Y_{01})	0.530142688	0.530143596	0.529981476
α_e ($-Y_{11}$)	2.97811496E-03	2.97804144E-03	2.97851063E-03
γ_e (Y_{21})	−9.17531E-06	−9.0881E-06	−9.02866E-06

3. Discussion

The $X^3\Delta$ constants used in our analysis were calculated using the isotopic relationships. The reliability of these constants can be assessed by comparison with recent independent measurements. Lincowski et al. [23] published B, D, A_D and λ_D spectroscopic constants for the $X^3\Delta$ $v = 0$ state for all four minor isotopologues from pure rotational transitions. The published constants were based on about 10 submillimeter lines for each isotopologue. The two sets of constants are shown for comparison in Table 5.

In addition, Breier et al. [24] conducted a mass-independent analysis of the isotopologues of TiO, recording over 130 pure rotational transitions in the $X^3\Delta$ state in the mm wave region (below 20 cm^{-1}) using a laser ablation source. That work was followed by Witsch et al. [25] also using a laser ablation source to record rovibrational lines in the $X^3\Delta$ state around 1000 cm^{-1}. Both papers published mass-independent constants for the TiO $X^3\Delta$ state.

Those constants were converted to Dunham parameters using the equation using Eq. (1) in Breier et al. [24]. A comparison of the equilibrium constants extracted from those two papers with the calculated $X^3\Delta$ state equilibrium constants used in this work are shown in Table 6 with satisfactory agreement.

A limited comparison was also made between the line list produced by this research and the ExoMol TiO line list [6]. A section of the spectrum was chosen between 14,145 and 14,169 cm^{-1} to match Fig. 11 in McKemmish et al.'s paper [6]. That region of the spectrum contains the 0–0 band of the $A^3\Phi$-$X^3\Delta$ transition and includes lines from all four minor isotopologues, predominantly R and Q branch lines, with J ranging from 11 to 45. 71 lines were compared with an average difference of 0.015 cm^{-1} suggesting the reliability of the ExoMol calculations.

4. Conclusion

A new line list for the TiO minor isotopologues for the $A^3\Phi$-$X^3\Delta$ transition has been produced from the TiO emission spectrum recorded in 1985 at the McMath-Pierce Solar Telescope. The list strengthens current experimental TiO line lists and has also produced spectroscopic constants for all four minor isotopologues in the $v = 0$ $A^3\Phi$ state. The isotopologue line lists for v'=0 and v''=0–4 are available as supplemental files.

The National Solar Observatory (NSO) is operated by the Association of Universities for Research in Astronomy, Inc. (AURA), under cooperative agreement with the National Science Foundation. Financial support was provided by the NASA Exoplanet Research Program (80NSSC21K0412). PB acknowledges RB for productive discussion.

Software: PGOPHER [17], Excel.

Data statement

Data are provided in the paper and in 7 supplementary tables.

Declaration of Competing Interest

The authors declare that they have no known competing financial interests or personal relationships that could have appeared to influence the work reported in this paper.

Data availability

All data is provided with the paper.

Supplementary materials

Supplementary material associated with this article can be found, in the online version, at doi:10.1016/j.jqsrt.2023.108745.

References

[1] Fowler A. The fluted spectrum of titanium oxide. Proc R Soc Lond 1907;A79: 509–18. https://doi.org/10.1098/rspa.1907.0059.
[2] Bochanski JJ, West AA, Hawley S, Covey KR. Low-mass dwarf template spectra from the Sloan Digital Sky Survey. Astron J 2007;133(2):531. https://doi.org/10.1086/510240.
[3] Evans TM, Sing DK, Wakeford HR, Nikolov N, Ballester GE, Drummond B, Kataria T, Gibson NP, Amundsen DS, Spake J. Detection of H_2O and evidence for TiO/VO in an ultra-hot exoplanet atmosphere. Astrophys J Lett 2016;822(1):L4. https://doi.org/10.3847/2041-8205/822/1/L4.
[4] Nugroho SK, Kawahara H, Masuda K, Hirano T, T Kotani T, Tajitsu A. High-resolution spectroscopic detection of TiO and a stratosphere in the day-side of WASP-33b. Astron J 2017;154(6):221. https://doi.org/10.3847/1538-3881/aa9433.
[5] Danilovich T, Gottlieb CA, Decin L, Richards AMS, Lee KLK, Kaminski T, Patel NA, Young KH, Menten KM. Rotational spectra of vibrationally excited AlO and TiO in oxygen-rich stars. Astrophys J 2020;904:110. https://doi.org/10.3847/1538-4537/abc079.
[6] McKemmish LK, Masseron T, Hoeijmakers HJ, Pérez-Mesa V, Grimm SL, Yurchenko SN, Tennyson J. ExoMol molecular line lists–XXXIII. The spectrum of Titanium Oxide. Mon Not R Astron Soc 2019;488(2):2836–54. https://doi.org/10.1093/mnras/stz1818.
[7] Yurchenko SN, Lodi L, Tennyson J, Stolyarov AV. Duo: a general program for calculating spectra of diatomic molecules. Compu Phys Commun 2016;202: 262–75. https://doi.org/10.1016/j.cpc.2015.12.021.
[8] McKemmish LK, Masseron T, Sheppard S, Sandeman E, Schofield Z, Furtenbacher T, Császár AG, Tennyson T, Sousa-Silva C. MARVEL analysis of the measured high-resolution rovibronic spectra of $^{48}Ti^{16}O$. Astrophys J Suppl Ser 2017;228(2):15. https://doi.org/10.3847/1538-4365/228/2/15.
[9] Bittner DM, Bernath PF. Spectroscopic constants and line positions for TiO singlet states. Astrophys J 2018;236:46. https://doi.org/10.3847/1538-4365/aabfe8.
[10] Hodges JN, Bernath P. Fourier transform spectroscopy of the $C^3\Delta$–$X^3\Delta$ transition of TiO in support of exoplanet spectroscopy. Astrophys J 2018;863:36. https://doi.org/10.3847/1538-4357/aacf07.
[11] Bernath P. Measured optical absorption cross sections of TiO. Astrophys J 2020; 895:87. https://doi.org/10.3847/1538-4357/ab7cd0.
[12] Bernath P, Cameron W. Near-infrared opacity of late M dwarfs and hot Jupiters: the $E^3\Pi$–$X^3\Delta$ transition of TiO. Astrophys J 2020;904:24. https://doi.org/10.3847/1538-4357/abc24c.
[13] Cameron WD, Bernath P. Visible opacity of M dwarfs and hot Jupiters: the TiO B $^3\Pi$– X $^3\Delta$ band system. Astrophys J 2022;926:39. https://doi.org/10.3847/1538-4357/ac49f0.
[14] Hughes GL, Gibson BK, Carigi L, Sanchez-Blazquez P, Chavez JM, Lambert DL. The evolution of carbon, sulfur and titanium isotopes from high redshift to the local Universe. Mon Not R Astron Soc 2008;390(4):1710–8. https://doi.org/10.1111/j.1365-2966.2008.13870.x.
[15] Serindag DB, Snellen IA, Molliere P. Measuring titanium isotope ratios in exoplanet atmospheres. Astron Astrophys 2021;655:A69. https://doi.org/10.1051/0004-6361/2021141941.
[16] Pavlenko YV, Yurchenko SN, McKemmish LK, Tennyson J. Analysis of the TiO isotopologues in stellar optical spectra. Astron Astrophys 2020;642:A77. https://doi.org/10.1051/0004-6361/202037863.
[17] Western CM. PGOPHER: a program for simulating rotational, vibrational and electronic spectra. J Quant Spectrosc Rad Transf 2017;186:221–42. https://doi.org/10.1016/j.jqsrt.2016.04.010.
[18] Barnes M, Merer AJ, Metha GF. Rotational and hyperfine structure of some low-J lines in the $A^3\Phi$-$X^3\Delta$ (0,0) band of TiO. J Molec Spectrosc 1996;180:437–40. https://doi.org/10.1006/jmsp.1996.0269.
[19] Ram RS, Bernath PF, Dulick M, Wallace L. The $A^3\Phi$ - $X^3\Delta$ (γ Bands) of TiO: laboratory and sunspot measurements. Astrophys J Suppl Ser 1999;(122):331–53. https://doi.org/10.1086/313212.
[20] Bernath PF. Spectra of atoms and molecules. 4th ed. New York, NY: Oxford University Press; 2020.
[21] Le Roy RJ. A computer program implementing the first-order RKR method for determining diatomic molecule potential energy functions. J Quant Spectrosc Rad Transf 2017;186:158–66. https://doi.org/10.1016/j.jqsrt.2016.03.030.
[22] Le Roy RJ. A computer program for solving the radial Schrödinger equation for bound and quasibound levels. J Quant Spectros Rad Transf 2017;186:167–78. https://doi.org/10.1016/j.jqsrt.2016.05.028.
[23] Lincowski AP, Halfen DT, Ziurys LM. Millimeter/Submillimeter spectroscopy of TiO ($X^3\Delta_r$): the rare titanium isotopologues. Astrophys J 2016;833:9. https://doi.org/10.3847/0004-637X/833/1/9.
[24] Breier AA, Wassmuth B, Fuchs GW, Gauss J, Giesen TF. Mass-independent analysis of the stable isotopologues of gas-phase titanium monoxide - TiO. J Mol Spectrosc 2019;355:46–58. https://doi.org/10.1016/j.jms.201811.006.
[25] Witsch D, Breier AA, Doring E, Yamada KMT, Giesen TF, Fuchs GW. The rotationally resolved infrared spectrum of TiO and its isotopologues. J Molec Spectrosc 2021;377. https://doi.org/10.1016/j.jms.2021.111439.